

**Electronic Supplementary Information**

**Highly dispersed redox-active polyoxometalates periodic deposition on multi-walled carbon nanotubes for boosting electrocatalytic triiodide reduction in dye-sensitized solar cells**

Ting Wang,<sup>§a</sup> Ming Xu,<sup>§a</sup> Xiaohong Li,<sup>a</sup> Chunlei Wang,<sup>b</sup> Weilin Chen<sup>\*a</sup>

<sup>a</sup>Key Laboratory of Polyoxometalate Science of Ministry of Education Department of Chemistry, Northeast Normal University, Changchun 130024, China. E-Mail: chenwl@nenu.edu.cn.

<sup>b</sup>Northeast Normal University Library, Changchun, 130024, China

<sup>§</sup>These two authors equally contributed to this paper.

## Table of Contents

<b>Supplementary Figures.....</b>	S3
Figure S1. IR spectra of POMs salts, POMs/CNTs nanocomposites employed as the CEs.....	S3
Figure S2. The PXRD patterns of (a, c, e, g) POMs salts; (b, d, f, h) POMs/CNTs nanocomposites employed as the CEs.....	S4
Figure S3. The EDX result of $\text{Co}_4\text{PW}_9/\text{CNTs}$ nanocomposites.....	S5
Figure S4. The full XPS spectra of (a) $\text{PW}_{12}/\text{CNTs}$ , (b) $\text{PMo}_{12}/\text{CNTs}$ , (c) $\text{P}_2\text{W}_{18}/\text{CNTs}$ and (d) $\text{P}_2\text{Mo}_{18}/\text{CNTs}$ nanocomposites.....	S5
Figure S5. High-resolution XPS spectra of (a) W and (b) C in $\text{PW}_{12}/\text{CNTs}$ nanocomposite.....	S5
Figure S6. High-resolution XPS spectra of (a) Mo and (b) C in $\text{PMo}_{12}/\text{CNTs}$ nanocomposite.....	S6
Figure S7. High-resolution XPS spectra of (a) W and (b) C in $\text{P}_2\text{W}_{18}/\text{CNTs}$ nanocomposite.....	S6
Figure S8. High-resolution XPS spectra of (a) Mo and (b) C in $\text{P}_2\text{Mo}_{18}/\text{CNTs}$ nanocomposite.....	S6
Figure S9. The EDX results of (a) $\text{PW}_{12}/\text{CNTs}$ , (b) $\text{PMo}_{12}/\text{CNTs}$ , (c) $\text{P}_2\text{W}_{18}/\text{CNTs}$ and (d) $\text{P}_2\text{Mo}_{18}/\text{CNTs}$ nanocomposites.....	S7
Figure S10. The cross sectional view of the $\text{Co}_4\text{PW}_9/\text{CNTs}$ CE.....	S7
Figure S11. The SEM images of (a) $\text{PW}_{12}/\text{CNTs}$ , (b) $\text{PMo}_{12}/\text{CNTs}$ , (c) $\text{P}_2\text{W}_{18}/\text{CNTs}$ and (d) $\text{P}_2\text{Mo}_{18}/\text{CNTs}$ nanocomposites.....	S7
Figure S12. The TEM images of (a) $\text{PW}_{12}/\text{CNTs}$ , (b) $\text{PMo}_{12}/\text{CNTs}$ , (c) $\text{P}_2\text{W}_{18}/\text{CNTs}$ and (d) $\text{P}_2\text{Mo}_{18}/\text{CNTs}$ nanocomposites.....	S8
Figure S13. The equivalent circuit for EIS analysis; $R_s$ is the series resistance, CPE represents the electrochemistry double-layer capacitance, the charge transfer resistance related to the IRR process is $R_{ct}$ .....	S8
Figure S14. Long-term stability of a DSSC based on $\text{Co}_4\text{PW}_9/\text{CNTs}$ CE.....	S9
<b>Supplementary Tables.....</b>	S10
Table S1. The POMs salts employed as the CEs in this study.....	S10
Table S2. Electrochemical parameters for different CEs.....	S10
<b>References.....</b>	S10

## Supplementary Figures

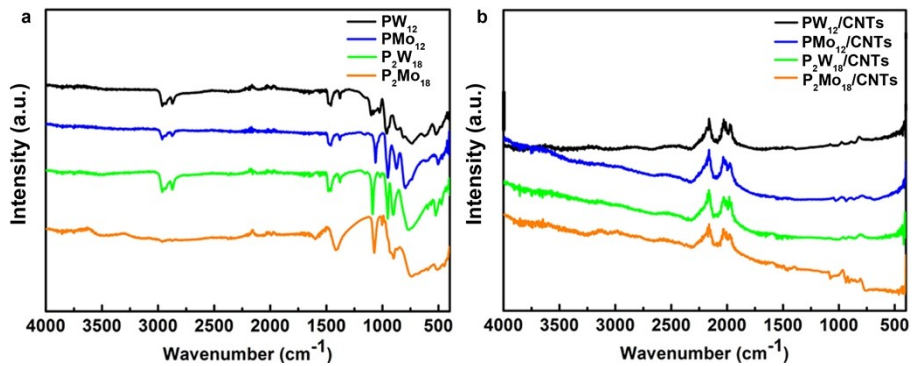


**Fig. S1.** IR spectra of POMs salts, POMs/CNTs nanocomposites employed as the CEs.

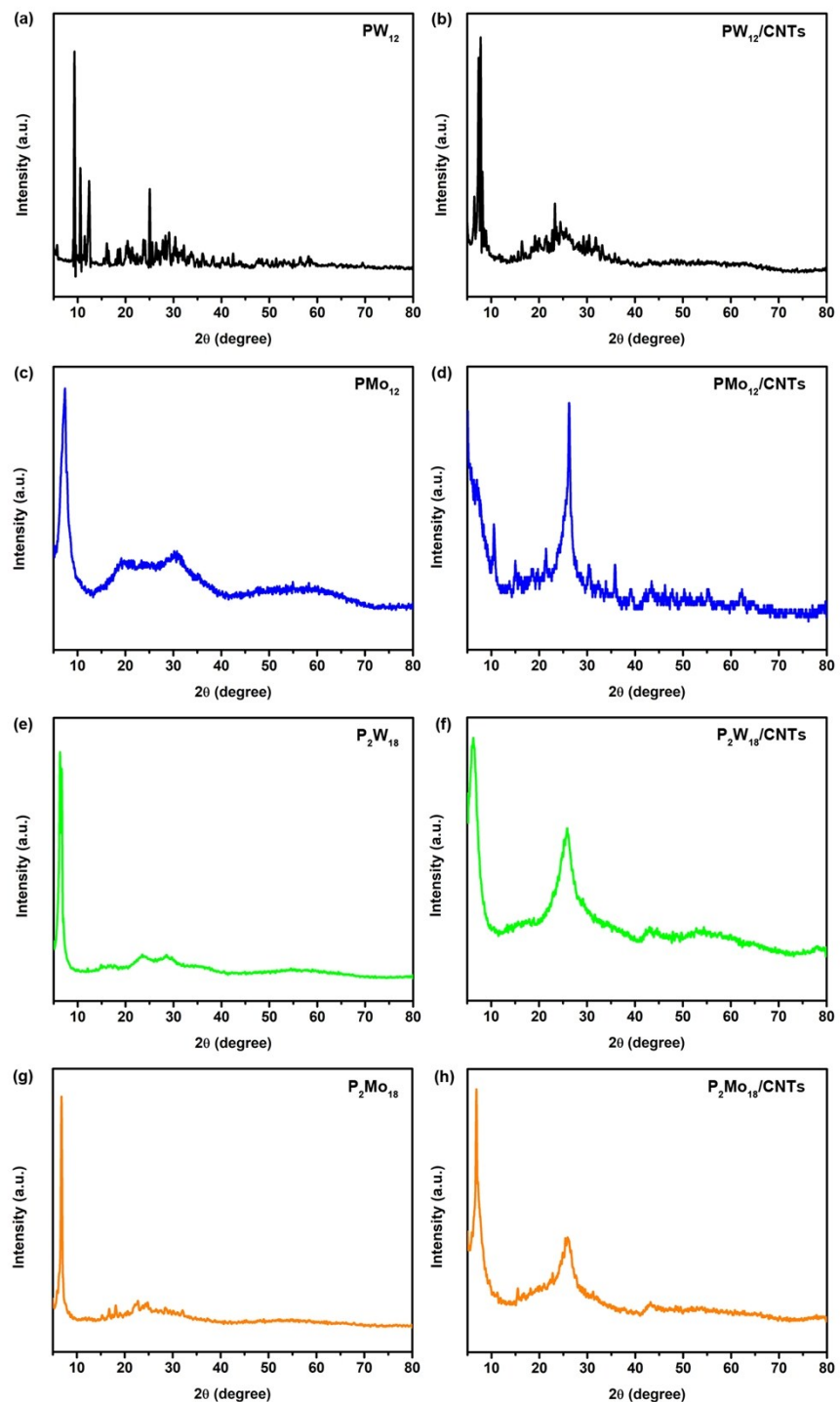


**Fig. S2.** The PXRD patterns of (a, c, e, g) POMs salts; (b, d, f, h) POMs/CNTs nanocomposites employed as the CEs.

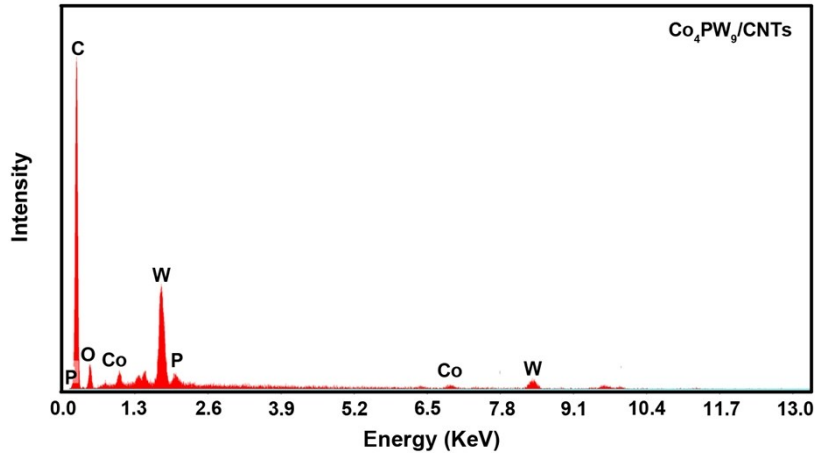


**Fig. S3.** The EDX result of  $\text{Co}_4\text{PW}_9/\text{CNTs}$  nanocomposites.

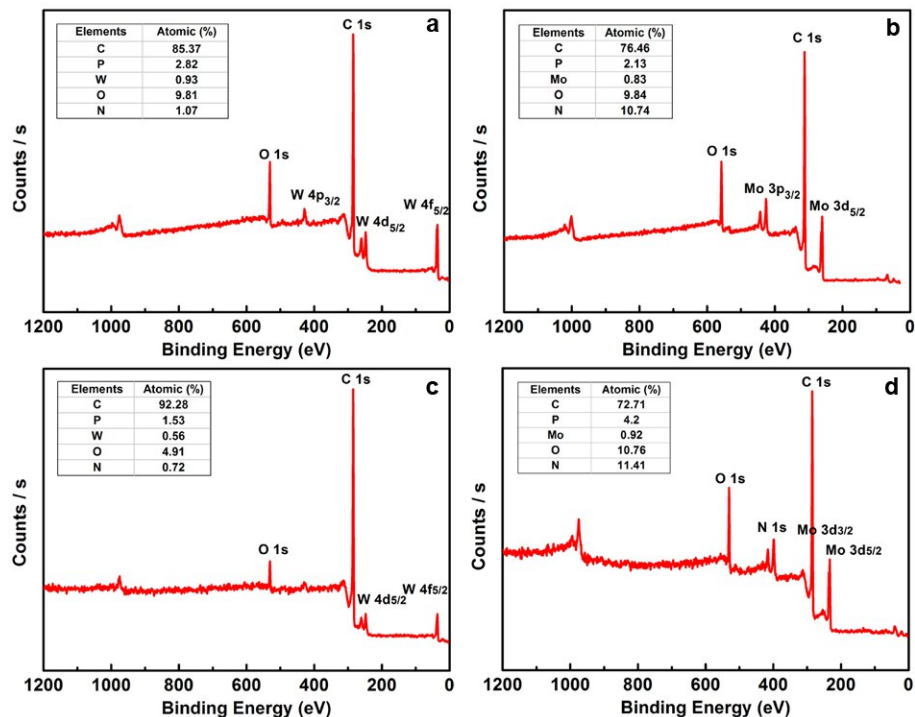


**Fig. S4.** The full XPS spectra of (a) PW<sub>12</sub>/CNTs, (b) PMo<sub>12</sub>/CNTs, (c) P<sub>2</sub>W<sub>18</sub>/CNTs and (d) P<sub>2</sub>Mo<sub>18</sub>/CNTs nanocomposites.

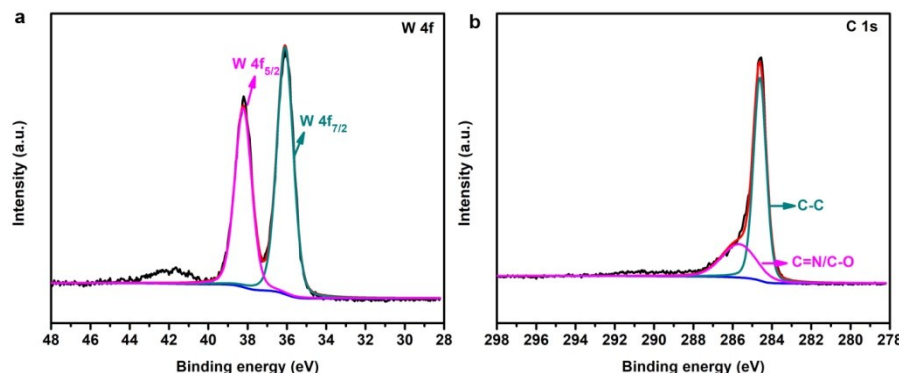


**Fig. S5.** High-resolution XPS spectra of (a) W and (b) C in PW<sub>12</sub>/CNTs nanocomposite.

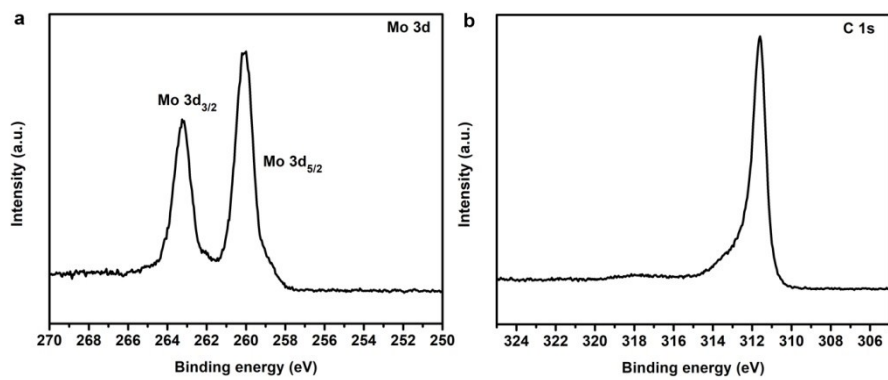


**Fig. S6.** High-resolution XPS spectra of (a) Mo and (b) C in PMo<sub>12</sub>/CNTs nanocomposite.

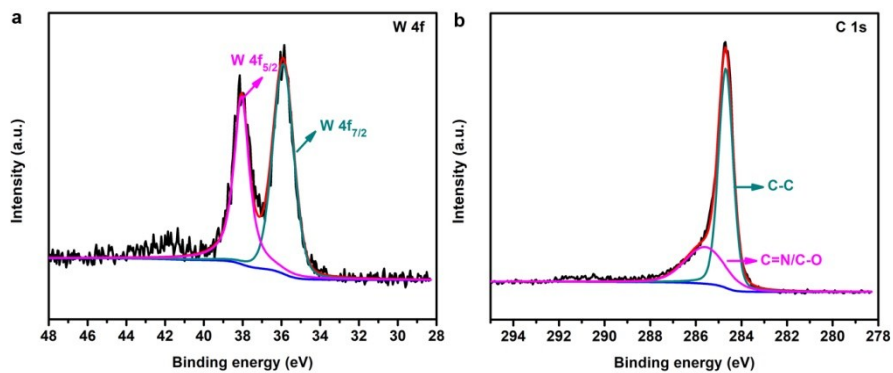


**Fig. S7.** High-resolution XPS spectra of (a) W and (b) C in P<sub>2</sub>W<sub>18</sub>/CNTs nanocomposite.

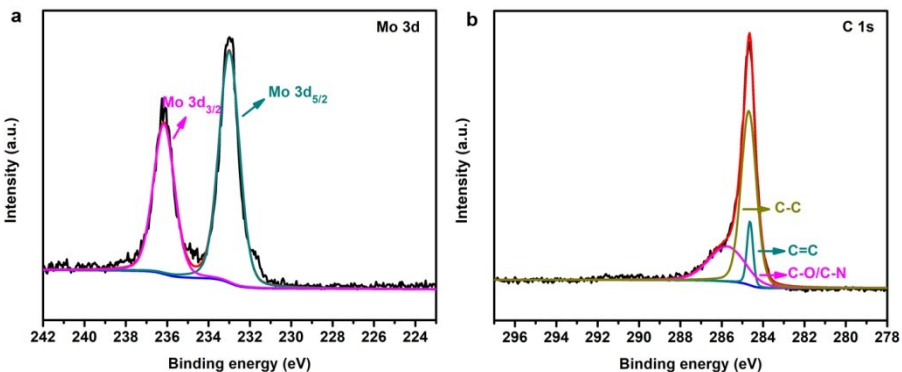


**Fig. S8.** High-resolution XPS spectra of (a) Mo and (b) C in P<sub>2</sub>Mo<sub>18</sub>/CNTs nanocomposite.

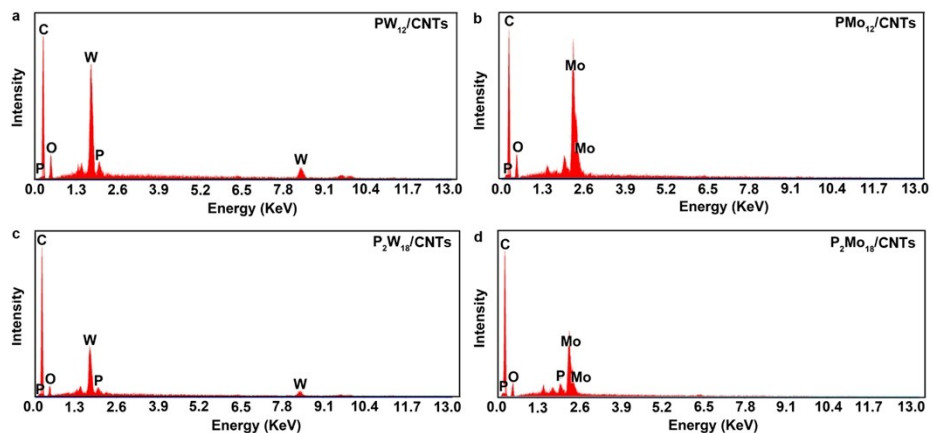


**Fig. S9.** The EDX results of (a) PW<sub>12</sub>/CNTs, (b) PMo<sub>12</sub>/CNTs, (c) P<sub>2</sub>W<sub>18</sub>/CNTs and (d) P<sub>2</sub>Mo<sub>18</sub>/CNTs nanocomposites.

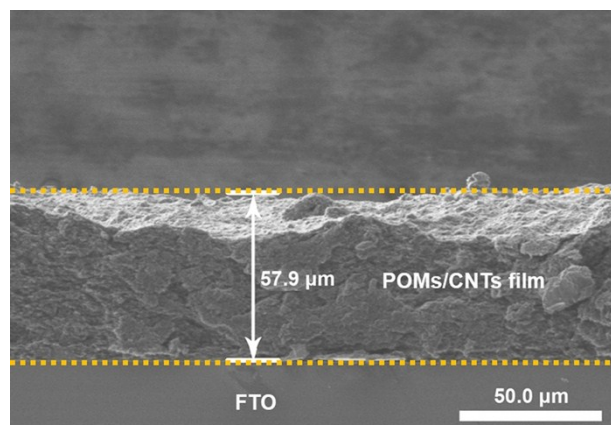


**Fig. S10.** The cross sectional view of the Co<sub>4</sub>PW<sub>9</sub>/CNTs CE.

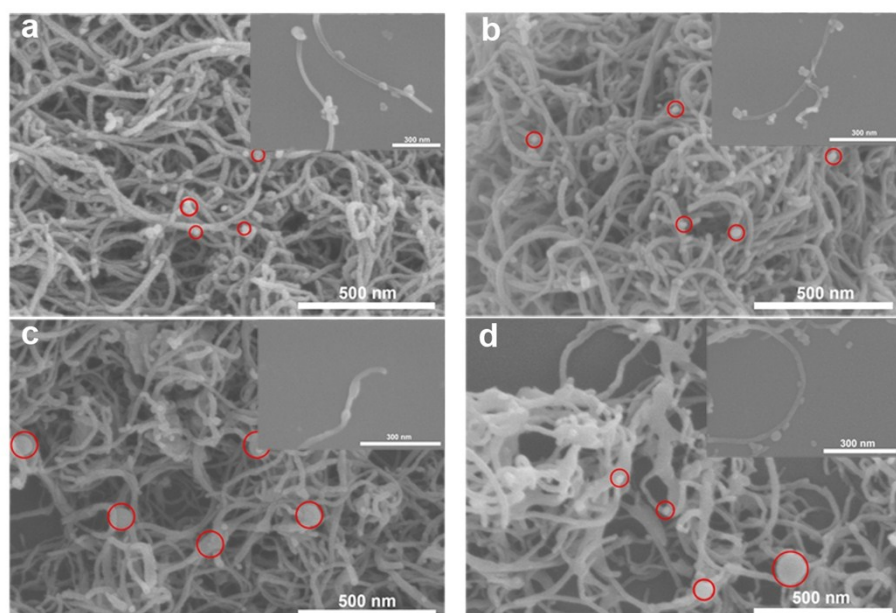


**Fig. S11.** The SEM images of (a) PW<sub>12</sub>/CNTs, (b) PMo<sub>12</sub>/CNTs, (c) P<sub>2</sub>W<sub>18</sub>/CNTs and (d) P<sub>2</sub>Mo<sub>18</sub>/CNTs nanocomposites.

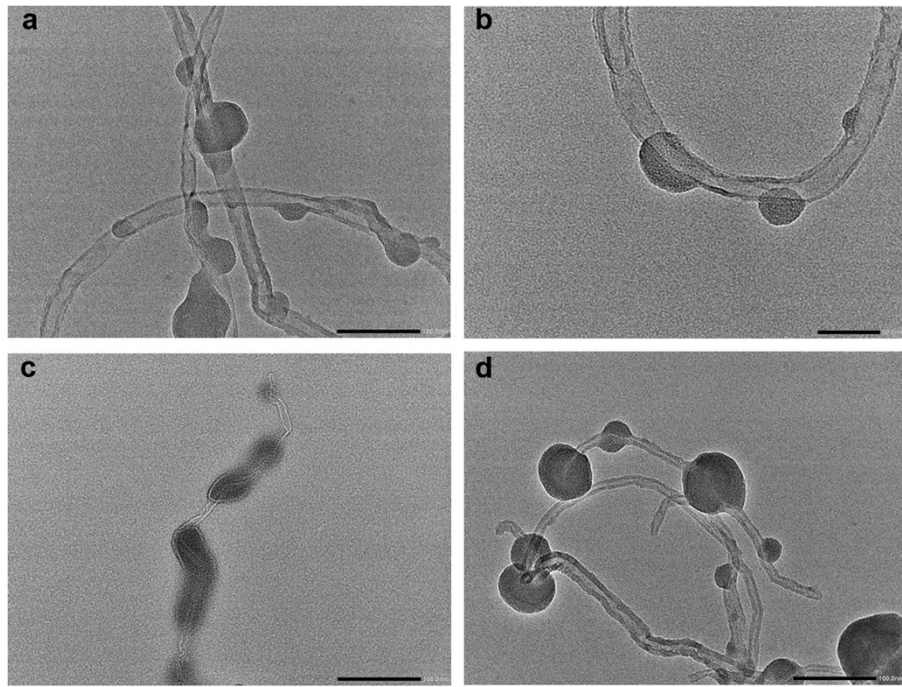


**Fig. S12.** The TEM images of (a)  $\text{PW}_{12}/\text{CNTs}$ , (b)  $\text{PMo}_{12}/\text{CNTs}$ , (c)  $\text{P}_2\text{W}_{18}/\text{CNTs}$  and (d)  $\text{P}_2\text{Mo}_{18}/\text{CNTs}$  nanocomposites.

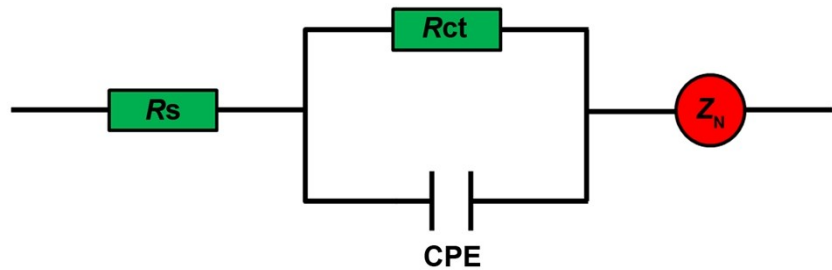


**Fig. S13.** The equivalent circuit for EIS analysis;  $R_s$  is the series resistance, CPE represents the electrochemistry double-layer capacitance, the charge transfer resistance related to the IRR process is  $R_{ct}$ .

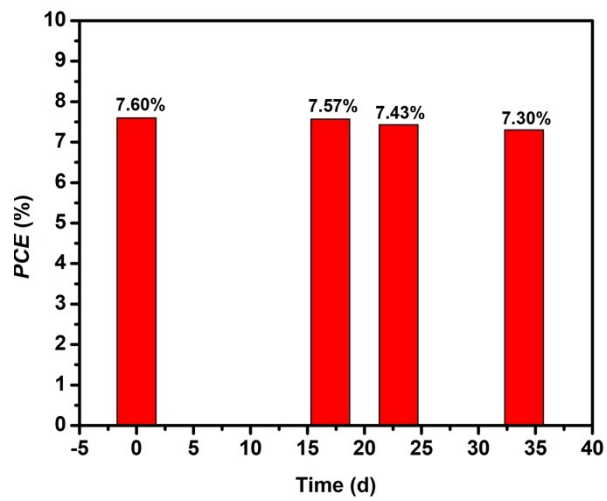


**Fig. S14.** Long-term stability of a DSSC based on  $\text{Co}_4\text{PW}_9/\text{CNTs}$  CE.

## Supplementary Tables

**Table S1.** The POMs salts employed as the CEs in this study.

Entry no	POMs salts	Abbreviation	Ref.
1	TBA <sub>3</sub> [PW <sub>12</sub> O <sub>40</sub> ] <sup>a</sup>	PW <sub>12</sub>	[1]
2	TBA <sub>3</sub> [PMo <sub>12</sub> O <sub>40</sub> ]	PMo <sub>12</sub>	[2]
3	TBA <sub>6</sub> [P <sub>2</sub> W <sub>18</sub> ]	P <sub>2</sub> W <sub>18</sub>	[3]
4	TBA <sub>6</sub> [P <sub>2</sub> Mo <sub>18</sub> ]	P <sub>2</sub> Mo <sub>18</sub>	[4]
5	Na <sub>10</sub> [Co <sub>4</sub> (H <sub>2</sub> O) <sub>2</sub> (PW <sub>9</sub> O <sub>34</sub> ) <sub>2</sub> ] · 27H <sub>2</sub> O	Co <sub>4</sub> PW <sub>9</sub>	[5]

[a] TBA: tetra-n-butylammonium.

**Table S2.** Electrochemical parameters for different CEs.

CEs	R <sub>s</sub> (Ω·cm <sup>2</sup> )	R <sub>ct</sub> (Ω·cm <sup>2</sup> )	J <sub>Red</sub> (mA cm <sup>-2</sup> )	E <sub>pp</sub> (mV)	f <sub>max</sub> (Hz)	τ(μs)
Pt	10.54	13.50	-3.16	900	2234.36	71.27
CNTs	19.04	24.04	-1.47	740	19.96	7977.66
PW <sub>12</sub> /CNTs	11.03	10.90	-3.50	600	5067.43	31.42
PMo <sub>12</sub> /CNTs	11.05	15.50	-6.18	280	5937.08	26.82
P <sub>2</sub> W <sub>18</sub> /CNTs	11.56	6.97	-2.81	560	1320.82	120.56
P <sub>2</sub> Mo <sub>18</sub> /CNTs	10.48	10.85	-3.20	690	3593.43	44.31
Co <sub>4</sub> PW <sub>9</sub> /CNTs	11.75	1.20	-8.43	230	7316.63	21.76

## References

- [1] C. Sanchez, J. Livage, J. P. Launay and Y. Jeannin, Electron delocalization in mixed-valence molybdenum polyanions, *J. Am. Chem. Soc.*, 1982, **104**, 3194–3202.
- [2] G. A. Tsigdinos and C. J. Hallada, Molybdovanadophosphoric acids and their salts. I. Investigation of methods of preparation and characterization, *Inorg. Chem.*, 1968, **7**, 437–441.
- [3] R. Contant, W. G. Klemperer and O. Yaghi, Potassium octadecatungstodiphosphates (V) and related lacunary compounds, *Synth. Chem.*, 1990, **27**, 104–111.
- [4] J. F. Garvey and M. T. POPE, Chirality of oxidized and reduced octadecamolybdodiphosphate anions. Observation of a Pfeiffer effect, *Inorg. Chem.*, 1978, **17**, 1115–1117.
- [5] Q. S. Yin, J. M. Tan, C. Besson and C. L. Hill, A Fast Soluble Carbon-Free Molecular Water Oxidation Catalyst Based on Abundant Metals, *Science*, 2010, **328**, 342–345.